Simultaneous Estimation of Physiological Parameters and the Input Function—*In vivo* PET Data

Koon-Pong Wong, *Member, IEEE*, (David) Dagan Feng, *Senior Member, IEEE*, Steven R. Meikle, *Senior Member, IEEE*, and Michael J. Fulham

***Abstract*—Dynamic imaging with positron emission tomography (PET) is widely used for the *in vivo* measurement of regional cerebral metabolic rate for glucose (rCMRGlc) with [^{18}F]fluorodeoxy-D-glucose (FDG) and is used for the clinical evaluation of neurological disease. However, in addition to the acquisition of dynamic images, continuous arterial blood sampling is the conventional method to obtain the tracer time-activity curve in blood (or plasma) for the numeric estimation of rCMRGlc in mg glucose/100-g tissue/min. The insertion of arterial lines and the subsequent collection and processing of multiple blood samples are impractical for clinical PET studies because it is invasive, has the remote, but real potential for producing limb ischemia, and it exposes personnel to additional radiation and risks associated with handling blood. In this paper, based on our previously proposed method for extracting kinetic parameters from dynamic PET images, we developed a modified version (post-estimation method) to improve the numerical identifiability of the parameter estimates when we deal with data obtained from clinical studies. We applied both methods to dynamic neurologic FDG PET studies in three adults. We found that the input function and parameter estimates obtained with our noninvasive methods agreed well with those estimated from the *gold standard* method of arterial blood sampling and that rCMRGlc estimates were highly correlated ($r = 0.973$). More importantly, no significant difference was found between rCMRGlc estimated by our methods and the gold standard method ($P > 0.16$). We suggest that our proposed noninvasive methods may offer an advance over existing methods.**

***Index Terms*—Arterial input function, cerebral glucose metabolism, dynamic imaging, [^{18}F]fluorodeoxy-D-glucose, noninvasive measurement, positron emission tomography.**

Manuscript received September, 1998; revised January, 2000. This work was supported by the National Health and Medical Research Council under Grant 980042.

K.-P. Wong was with the Department of Electronic and Information Engineering, The Hong Kong Polytechnic University, Hong Kong. He is now with the Biomedical and Multimedia Information Technology Group, Basser Department of Computer Science, The University of Sydney, Sydney, N.S.W. 2006, Australia and is also with the Department of PET and Nuclear Medicine, Royal Prince Alfred Hospital, Camperdown, Sydney, N.S.W. 2050, Australia (e-mail: kpong@cs.usyd.edu.au).

D. Feng is with the Biomedical and Multimedia Information Technology Group, Basser Department of Computer Science, The University of Sydney, Sydney, N.S.W. 2006, Australia and is also with the Centre for Multimedia Signal Processing, Department of Electronic and Information Engineering, The Hong Kong Polytechnic University, Hong Kong (e-mail: feng@cs.usyd.edu.au).

S. R. Meikle is with the Department of PET and Nuclear Medicine, Royal Prince Alfred Hospital, Camperdown, Sydney, N.S.W. 2050, Australia.

M. J. Fulham is with the Department of PET and Nuclear Medicine, Royal Prince Alfred Hospital, Camperdown, Sydney, N.S.W. 2050, Australia and is also with the Department of Medicine, The University of Sydney, Sydney, N.S.W. 2006, Australia.

Publisher Item Identifier S 1089-7771(01)01711-3.

I. Introduction

POSITRON emission tomography (PET) with [^{18}F]fluorodeoxy-D-glucose (FDG) has been widely used to study regional brain glucose metabolism in normal subjects and in patients with a variety of neurological conditions. The three-compartment tracer kinetic model was originally developed by Sokoloff *et al.* [1] to measure glucose metabolic rate in the albino rat and it was later validated in humans [2]–[4]. A drawback of this approach is measurement of the input function for the compartment model. The input function is generally obtained by sampling blood at the radial artery or from an arterialized vein in a hand [2]–[4]. Arterial blood sampling is not practicable in a clinical environment because it is invasive and has the potential for causing irreversible tissue ischemia. Further, it may not be tolerated by the patient if additional studies are required for longitudinal evaluation. It also exposes personnel who perform the blood sampling to additional radiation and the risks associated with handling patient blood [5].

Recently, effort has been directed toward reducing or obviating the need for arterial blood sampling. The arterialized–venous (a–v) method involves heating the hand in a hot water bath which then promotes shunting between the capillary and venous vascular bed to avoid the discomfort and risks associated with arterial cannulation [3]. However, this method requires prolonged hand warming to ensure adequate shunting, and it is very dependent upon the site chosen for the placement of the venous cannula and the rate of blood flow. The best results are usually obtained from a cannula that is placed in a large vein on the dorsum of the hand, typically in a muscular male. Furthermore, it does not avoid the need for frequent sampling. Phillips *et al.* reported a method that uses a limited number of arterial blood samples [6], however, their method relies on arterial catheterization. Takikawa *et al*. proposed a method that approximates the input function by the average obtained from a population sample of humans [7], but arterial (or a–v) sampling is still necessary for the determination of the population input function. Eberl *et al*. reported a similar approach to Takikawa *et al.*, but they obtained blood samples using an a–v approach [8]. The input function for an individual patient was scaled by calibrating a "standard" input curve with blood samples drawn at 10- and 45-min postinjection. These methods simplify the generation of quantitative data for neurological FDG PET studies, but they do not directly measure the input function in an individual, nor do they allow the estimation of the microparameters (rate constants) of

TABLE I
BRAIN STRUCTURES AND TISSUE TYPES USED FOR ROI ANALYSIS

Structure	Abbreviation	Structure	Abbreviation
Basal ganglia	BG	Cerebellum	CBL
Inferior temporal gyrus	ITG	Occipital association cortex	OAC
Parietal lobe	PA	Superior temporal gyrus	ST
Superior frontal	SF	Thalamus	TH
Visual cortex	VC	Cingulate gyrus	CG
Grey matter*	GM	White matter*	WM
Whole brain*	WB	Hemisphere (White)*	HW
Lenticular nuclei*	LN		

*denotes the ROIs used for modeling with SIME

the FDG model. Furthermore, all these approaches would require repeated measurements in a group of patients or volunteers each time a new tracer or different infusion rate is used. A technique that was not invasive, practical to implement, and accurate would have advantages for the routine measurement of cerebral glucose metabolism in the clinic.

We recently proposed a modeling approach that estimates the input function and determines the physiological parameters simultaneously from several tissue time-activity curves (TACs). We evaluated this technique in computer simulations [9]. However, this method has not yet been tested in clinical studies. In this paper, we report our preliminary data with this method in dynamic neurologic FDG PET studies in three adults and propose a modified method (post-estimation method), which improves the standard deviation (SD) of parameter estimates. We also compare these two methods to the *gold standard* method in which continuous arterial blood samples are taken.

II. MATERIALS AND METHODS

A. Human Studies

Dynamic FDG PET studies were performed on three human subjects. One had refractory epilepsy and two were normal volunteers. All studies were performed at the National PET/Cyclotron Center, Taipei Veterans General Hospital, Taiwan, R.O.C. The studies were approved by the Institution Review Board. The PET scans were performed with a PC4096-15WB PET tomograph (GE/Scan-ditronix) that has eight rings and provides 15 slices with axial and transaxial resolutions of 6.5-mm full width at half maximum (FWHM) in the center of the field of view (FOV). The subjects fasted overnight before the study. A 15-min transmission scan was performed using rotating rod sources of ^{68}Ge for attenuation correction prior to intravenous administration of approximately 370 MBq FDG. The PET studies were performed for 2-h post injection. However, for the purpose of this study, only the first 60 min of data were used since this is a more practical and commonly employed protocol in other PET centers. During the first 60 min, 18 arterial blood samples were collected every 15-s from 0- to 2-min post injection; every 30-s from 2 to 3.5 min; and at 7, 10, 15, 20, 30, and 60 min. The samples were immediately placed on ice and the plasma was subsequently separated for the determination of FDG and glucose concentrations. The scanning schedule for the dynamic FDG PET studies during the first 60 min was: ten 12-s scans, two 30-s scans, two 1-min scans, one 1.5-min scan, one 3.5-min scan, two 5-min scans, one 10-min scan, and one 30-min scan. The acquired PET data were also decay corrected to the time of injection. The tomographic images were reconstructed using filtered back-projection with a Hann filter (cutoff frequency $= 0.5$ of the Nyquist frequency). Fifteen regions of interest (ROIs) of irregular shape and size were manually drawn over the PET images to obtain the tissue TACs for each subject. Table I tabulates the names and abbreviations of the brain structures and tissue types selected for the ROIs. The ROIs selected for modeling with the proposed method were based on visual identification of their corresponding TACs [9].

B. FDG Model

The differential equations that describe the FDG three-compartment model are expressed as follows [3], [4]:

$$\frac{d}{dt}c_e^*(t) = k_1^* c_p^*(t) - (k_2^* + k_3^*)c_e^*(t) + k_4^* c_m^*(t) \quad (1)$$

$$\frac{d}{dt}c_m^*(t) = k_3^* c_e^*(t) - k_4^* c_m^*(t) \quad (2)$$

$$c_i^*(t) = c_e^*(t) + c_m^*(t) \quad (3)$$

where $c_p^*(t)$, $c_e^*(t)$, and $c_m^*(t)$ represent FDG concentration in the plasma, FDG concentration in the tissue, and FDG-6-phosphate (FDG-6-P) concentration in the tissue, respectively. The rate constants in the model are k_1^* (min^{-1}) for forward transport of the FDG to tissue, k_2^* (min^{-1}) for reverse transport of FDG from the tissue to plasma, k_3^* (min^{-1}) for phosphorylation of FDG to FDG-6-P in tissue and k_4^* (min^{-1}) for dephosphorylation of FDG-6-P to FDG in tissue. The actual tissue activity c_T^* measured by PET can be expressed as

$$c_T^*(t) = (1 - \mathrm{CBV}) \cdot c_i^*(t) + \mathrm{CBV} \cdot c_p^*(t) \quad (4)$$

where $c_i^*(t)$ is the total tissue activity, and CBV (mL/100 g or %vol) is the fractional cerebral blood volume, which accounts for the vascular contribution in the tissue ROI [10], [11]. The regional cerebral metabolic rate for glucose (rCMRGlc) is calculated according to the following equation [3], [4]:

$$\mathrm{rCMRGlc} = \frac{k_1^* k_3^*}{k_2^* + k_3^*}\frac{\mathrm{Cglc}}{\mathrm{LC}} \equiv K\frac{\mathrm{Cglc}}{\mathrm{LC}} \quad (5)$$

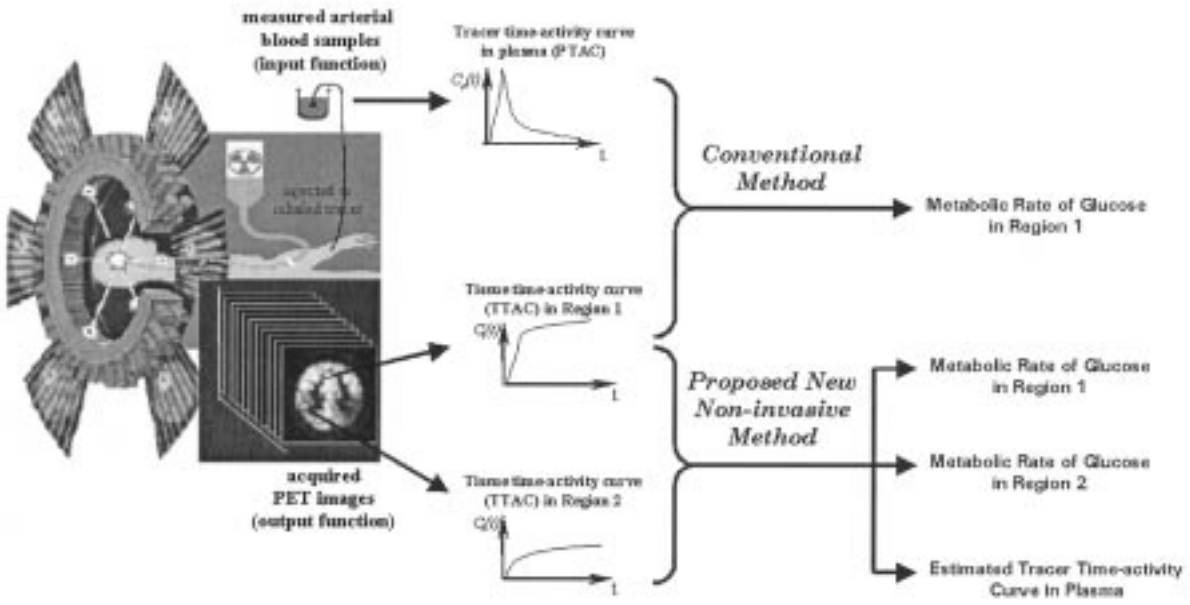

Fig. 1. Comparison of the conventional kinetic approach and the proposed noninvasive method. The conventional approach requires to utilize TACs in plasma and tissue. On the other hand, the proposed method requires the tissue TACs in two or more regions.

where Cglc is the glucose concentration in plasma, and LC is the lumped constant that embodies the difference between FDG and glucose in transportation and phosphorylation [3], [4]. The macro-parameter $K(= k_1^* k_3^*/(k_2^* + k_3^*))$ is proportional to rCMRGlc and to the uptake of FDG. In this paper, rCMRGlc (or, equivalently, K) is one of the main parameters used to evaluate the accuracy of our proposed method.

C. Conventional Kinetic Method

In the conventional kinetic approach, the rate constants in the kinetic model are determined by nonlinear least squares (NLLS) fitting to the tissue TAC [4]. The model differential equations (2) and (3) are solved and a convolution integral equation that represents the tissue TAC is formulated [3], [4]. NLLS is then employed to minimize the errors between the convolution integral equation and the observed PET measurements. Note that the formulation of the convolution integral equation requires knowledge of the input function $c_p^*(t)$, which is obtained by continuously measuring the arterial or a–v blood samples.

D. Noninvasive Approach

We have previously reported [9] the identifiability, reliability, and Monte Carlo simulations of our proposed method and only a brief summary of the method is presented here. Multiple tissue TACs can be obtained by defining different ROIs on the dynamic PET images (shown in Fig. 1). These TACs are the convolution of the input function with the physiological impulse response functions (IRFs) corresponding to the ROIs. The input function and the IRF parameters may thus be estimated simultaneously from two or more tissue TACs. We refer to this method as simultaneous estimation (SIME).

The input function and physiological parameters of the IRFs were derived by the conventional kinetic approach and SIME. A input function model for bolus administration of FDG [12] was used in SIME to describe the (estimated) arterial input function and to reduce the uncertainties in parameter estimates [13], [14]. The mathematical expression for this model without the delay factor is given by

$$c_p^*(t) = (A_1 t - A_2 - A_3)e^{\lambda_1 t} + A_2 e^{\lambda_2 t} + A_3 e^{\lambda_3 t} \quad (6)$$

where A_1 (in μCi/mL/min), A_2 and A_3 (in μCi/mL) are the coefficients of the model; λ_1, λ_2 and λ_3 (in min^{-1}) are the eigenvalues of the model. These parameters are determined by least squares fitting the blood samples in the conventional kinetic method and SIME.

In the input function, the last exponential described by the parameters A_3 and λ_3 in (6) dominates the tail of the blood curve. We have shown in our computer simulation study that using two late venous samples as the *a priori* knowledge for the input function can markedly improve the identifiability and reliability of SIME [9]. In this paper, a similar strategy was adopted. However, instead of fixing A_3 and λ_3 to certain assumed values, as we did in our simulation [9], two venous blood samples (30- and 60-min postinjection) were taken to determine A_3 and λ_3.

Having defined the last exponential of the input function and the ROIs whose TACs were used for modeling, NLLS was used in SIME to determine the input function and the IRF parameters by minimizing the following cost function:

$$\Phi(\theta) = \sum_{i=1}^{N}\sum_{j=1}^{M}\left[\left(\hat{c}_p^*(t) \otimes h_i(t)\right) \otimes \delta\left(t - t_j'\right) - c_{T_i}^*\left(t_j'\right)\right]^2 + \sum_{k=1}^{m} w_k\left[\hat{c}_p^*(t_k) - \overline{c}_p^*(t_k)\right]^2 \quad (7)$$

where N is the total number of ROIs incorporated into the model fitting procedure, M is the number of frames for each tissue TAC, $h_i(t)$ is the IRF of the ith ROI with microparameters $k_1^* - k_4^*$ and CBV, θ denotes the vector of parameters to be estimated and it is formed by concatenating several sets of rate

constant parameters $[k_1^*, k_2^*, k_3^*, k_4^*, \text{CBV}]^\top$ in different ROIs with the parameter vector $[A_1, \lambda_1, A_2, \lambda_2, A_3, \lambda_3]^\top$ of the input function, $\delta(t-t_j')$ is a Dirac delta function shifted in time by t_j' units, $\otimes$ is the convolution integral operator, $\hat{c}_p^*(t)$ is the estimated arterial input function, $\overline{c}_p^*(t_k)$ is the FDG concentration in plasma measured at time $t_k (k = 1, 2, \ldots, m)$, m is the number of venous blood samples taken late in the course of the study, and w_k is chosen to be 100 so that the samples from the blood [i.e. $\overline{c}_p^*(t_k)$] are given more weight, as they are usually less noisy (thus, more reliable) than PET measurements. In all of the studies, $\overline{c}_p^*(t_k)$ were measured by counting the radioactivity concentrations in the venous blood samples ($m = 2$) taken at 30- and 60-min postinjection in an NaI well counter that was cross-calibrated to the PET scanner.

E. Post-Estimation Technique

Although precise parameter estimates can be obtained theoretically with SIME, raw PET data are often extremely noisy due to issues such as photon attenuation, scatter, etc. The result is that the information matrix becomes poorly conditioned and the subsequent estimation of the SDs of the parameter estimates are poor. In addition, input/output scaling can also result in large SDs in the parameters because sensitivities of the input and output are not of the same order, which can produce near rank deficiency in the information matrix. The dimensions and the nonlinearity of parameter space can also affect the information matrix to a certain extent. In this situation, SIME may not be able to provide acceptable estimates of the SDs, though the values of the parameter estimates are accurate. Thus, we have introduced a technique that is applied after SIME, for situations where the parameter estimates have large SDs or coefficients of variation (CVs). We refer to this method as simultaneous estimation with post-estimation (SIMEP), which is based on the assumption that the input function obtained by SIME can globally minimize the errors between all of the measured data and the predicted tissue TACs by (7) in the least squares sense. The parameters in the IRFs can then be estimated separately by using the estimated input function and the individual tissue TACs as input–output pairs. The SDs of the parameters can be greatly improved due to the reduction in dimensionality of parameter space.

F. Data Analysis

The recovered (or estimated) input function obtained from SIME was compared to the measured arterial input function visually to see if there was any discrepancy. The areas under the measured and recovered input functions (AUCs) for the time from 0 to 2 min (where the peak occurs), for the time from 2 to 10 min (rapid washout), for the time from 10 to 30 min (slow washout), and for the time from 30 to 60 min (constant clearance), were computed using the trapezoidal method and compared. Compartmental model fitting with the use of the measured arterial blood samples as the input function (i.e., *gold standard* method) and with the use of the input function recovered by SIME (i.e., SIMEP) were then performed on the ten ROIs, which were not used in SIME and the corresponding rCMRGlc in each ROI was then estimated. Linear regression analysis was carried out to compare the estimates of rCMRGlc obtained from both methods for the ten ROIs tabulated in Table I for all subjects. Paired student's t test was performed on the 30 (three subjects $\times$ ten ROIs) rCMRGlc estimates to test the hypothesis that rCMRGlc estimates obtained from the invasive and SIMEP methods are not significantly different, and $P < 0.05$ was chosen as the significance level.

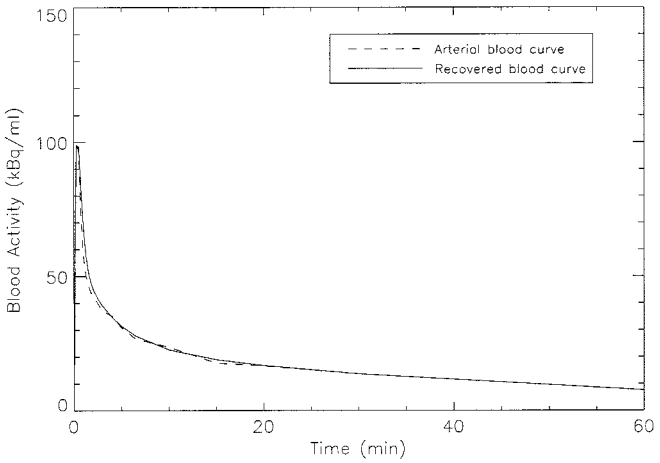

Fig. 2. Comparison of the measured arterial input function with the recovered input function for one subject. The recovered blood curve was obtained from simultaneously fitting three ROI TACs at a time.

For the tissue TACs that were used in SIME, we mainly looked at the parameter estimates and the SDs in the IRFs obtained with the invasive method, SIME, and SIMEP, respectively, to evaluate the identifiability and the reliability of SIME and to verify that more reliable results can be obtained with SIMEP. The SDs for the rate constants were the asymptotic SDs, which were given by the square roots of the diagonal elements of the asymptotic variance–covariance matrix (inverse of the Fisher Information matrix) of NLLS, while the precision of rCMRGlc was calculated by error propagation of the rate constants.

III. Results

A. Recovery of the Input Functions

Fig. 2 shows the measured and recovered input functions in one of the studies. The recovered blood curve was derived by minimizing the cost function with the tissue TACs obtained from three ROIs [grey matter (GM), white matter (WM), and whole brain (WB)]. It can be seen that there was very good agreement between the recovered and measured arterial blood curves. The difference between the two curves at the peak was only 2.5%. It was also found that the time at which the two input functions reach their peaks was almost identical. Similar results were obtained for all studies where the number of ROIs was more than two. However, in some cases, the peak estimation could be higher for the recovered input function. An example is shown in Fig. 3, where the result was obtained from another subject studied. The tissue TACs were also obtained from three ROIs (GM, WM, and WB). It is, however, important to note that the measured arterial input function may not necessarily be very accurate due to measurement noise.

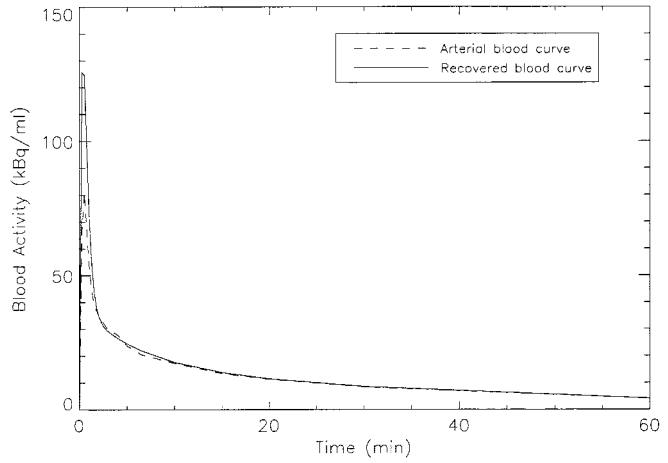

Fig. 3. Comparison of the measured arterial input function with the recovered input function for another subject studied. Again, the recovered blood curve was obtained from simultaneously fitting three ROI TACs at a time. However, the peak estimation was not as good as the one shown in Fig. 2.

Table II compares the AUCs of the measured arterial input functions and the recovered input functions at different time intervals of the experiment with different number of ROIs used in SIME. It can be seen that the areas covered by the measured arterial input functions and the recovered input functions for the period beyond 0–2 min were in very good agreement, despite the possible underestimation or overestimation within 0–2 min where peak occurs, due to underestimation or overestimation of the peaks. In general, the recovered input functions resembled their true measurements very well. Moreover, the ability of SIME to recover the input function was generally improved with increasing number of ROIs, as seen in Table II, provided that the tissue TACs used for modeling in SIME are distinct.

B. Estimation of the Physiological Parameters

Apart from the recovery of the arterial input function from the measured tissue TACs, the estimation of the physiological parameters and the rate constants are also of primary concern. Fig. 4 plots the measured tissue data (at mid-scan time) and the fitted curves by SIME, SIMEP, and the conventional kinetic (invasive) method, respectively. The results shown for SIME were obtained from fitting two ROIs (GM and WM) according to the cost function [see (7)]. It can be seen that the fitted curves were in good agreement with the measured data. Furthermore, the TACs predicted by the parameters obtained from SIME and SIMEP are almost identical, indicating that the main difference between SIME and SIMEP is in the parameter variances rather than the values themselves. Similar results were also found for all subjects with different number of ROIs included in the fitting procedure of SIME.

Figs. 5 and 6 plot the parameter estimates and the SDs (denoted by error bars) obtained with SIME, SIMEP, and the invasive method for the IRFs corresponding to the tissue types of GM and WM, respectively, in one of the subjects. As shown in the figures, we can obtain quite good estimates of rCMRGlc for GM and WM when compared to those estimated from the conventional kinetic method, even when only two ROIs are used in the model fitting procedure with SIME. However,

TABLE II
COMPARISON OF THE AREAS UNDER THE MEASURED AND RECOVERED INPUT FUNCTIONS (AUCs) FOR DIFFERENT TIME INTERVALS OF THE EXPERIMENT. VALUES APPEARING IN BOLD CORRESPOND TO THE AUCs COVERED BY THE MEASURED ARTERIAL BLOOD CURVES IN THE SUBJECTS

Subject	No. of ROIs	AUC at different time intervals			
		0–2 min	2–10 min	10–30 min	30–60 min
1	—	**101.934**	**186.040**	**237.013**	**188.756**
	2	117.075	188.060	282.713	213.499
	3	144.443	188.823	241.919	190.967
	4	92.596	189.550	238.612	190.213
	5	101.183	190.253	231.339	189.219
2	—	**114.101**	**203.028**	**300.459**	**270.618**
	2	136.062	230.050	308.530	278.353
	3	136.417	222.424	300.966	276.642
	4	141.672	223.816	296.257	274.805
	5	135.581	219.572	298.818	275.906
3	—	**122.156**	**240.408**	**341.510**	**320.235**
	2	131.465	244.662	346.714	320.383
	3	102.592	230.047	346.184	320.437
	4	110.419	240.534	349.918	320.620
	5	116.864	237.716	348.399	320.527

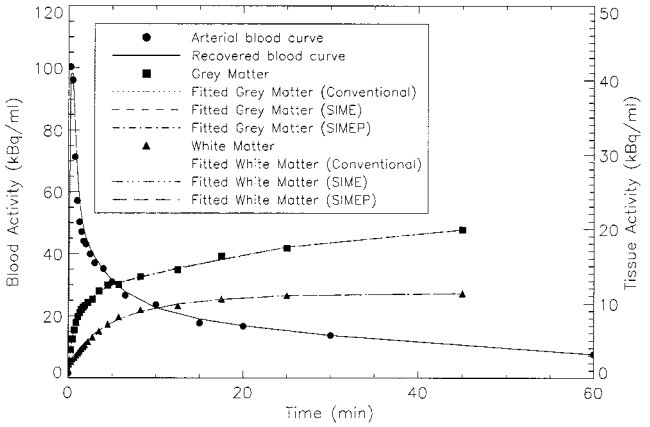

Fig. 4. Arterial blood samples, recovered input function, and predicted tissue TACs corresponding to GM and WM, respectively. The recovered input function was obtained by SIME using the TACs of the two tissue types mentioned above. The fitted curves for the tissue TACs were obtained with the conventional kinetic method using the arterial blood samples as the input function, with the recovered input function obtained with SIME and SIMEP, respectively

there was a poor estimation of SDs by SIME for some of the parameters in the IRFs, e.g., k_4^* and CBV. In addition, the estimated SDs obtained with SIME for the parameters may be very large [(standard deviation)/(parameter estimate) > 1, or equivalently, percent CV $> 100\%$], as shown in the figures, in which some of the error bars are extended beyond the maximum values of the graphs. When SIMEP is applied to these data, the values and SDs of the estimated parameters are generally improved as compared to those estimated by SIME and are comparable to those obtained with the conventional kinetic method.

Table III shows the comparison of CVs (in percentage) for rCMRGlc estimates in ten ROIs, obtained with the measured

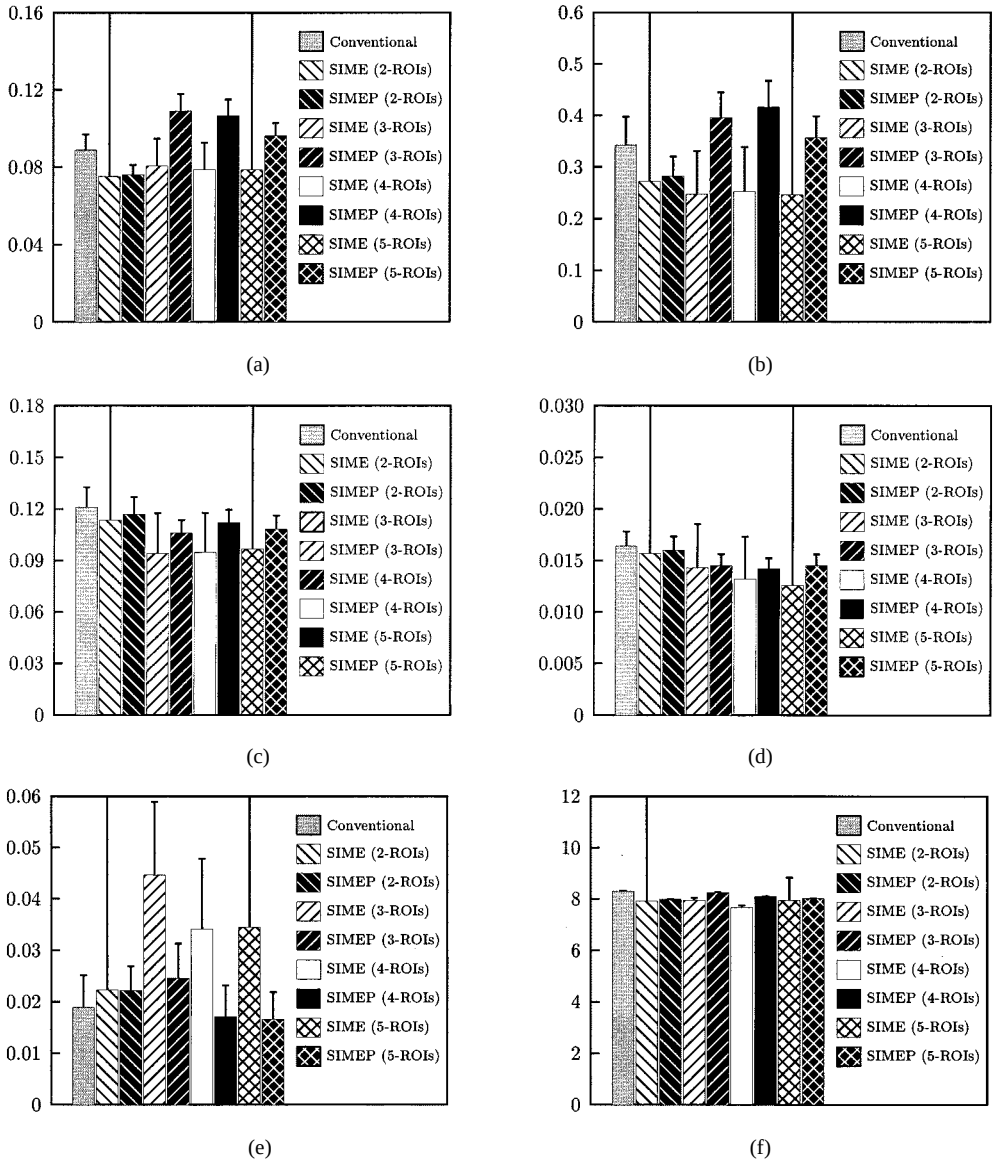

Fig. 5. Parameter estimates obtained with SIME, SIMEP, and the conventional kinetic method in GM. (a) $k_1^*\,(\mathrm{min}^{-1})$. (b) $k_2^*\,(\mathrm{min}^{-1})$. (c) $k_3^*\,(\mathrm{min}^{-1})$. (d) $k_4^*\,(\mathrm{min}^{-1})$. (e) CBV (mL/100 g). (f) rCMRGlc (mg/min/100 mL). In (a)–(f), error bars represent the SDs of the parameter estimates.

arterial blood samples as the input function and the recovered input function obtained with SIME (using three ROIs) for the three human subjects. The identifiability of the estimates obtained with the measured arterial input functions and the recovered input functions are almost the same. Linear regression analysis was carried out to compare rCMRGlc estimates obtained from our methods and from the invasive method. The results are shown in Fig. 7 where the estimates of rCMRGlc obtained with the *gold standard* method were plotted versus those obtained with SIME (using three ROIs) for different ROIs tabulated in Table I (excluding those used in SIME) for all subjects. It can be seen that rCMRGlc can be estimated reliably with the use of the recovered input functions (SIME, three ROIs). The slope of the regression line for rCMRGlc was close to one (1.009) and the intercept was nearly equal to zero (0.007), and there was very high correlation between the estimates obtained with both methods ($r = 0.973$, $P < 0.0001$). The agreement between the rCMRGlc estimates was further examined using paired student's t test. We found that the estimates obtained with the invasive and the proposed method (SIMEP with the input function obtained with SIME using three ROIs as an example) were not significantly different ($P = 0.16$, two-tailed test). Similar results were also found for all subjects with the number of ROIs included in the fitting procedure of SIME greater than two.

IV. Discussion

Our results show that the proposed methods are able to recover the input function from dynamic PET image data and to provide good parameter estimates when compared to the conventional kinetic method. The reliability of estimating physiological parameters was improved by our SIMEP method if $\geq$2 ROIs were used. Fewer ROIs ($<$3) still provided an accurate estimation of rCMRGlc, despite the differences between k_4^* and CBV estimates and the large variability in the rate constants.

Accurate quantification of rCMRGlc is directly related to the precise definition of the input function. The shape of the input

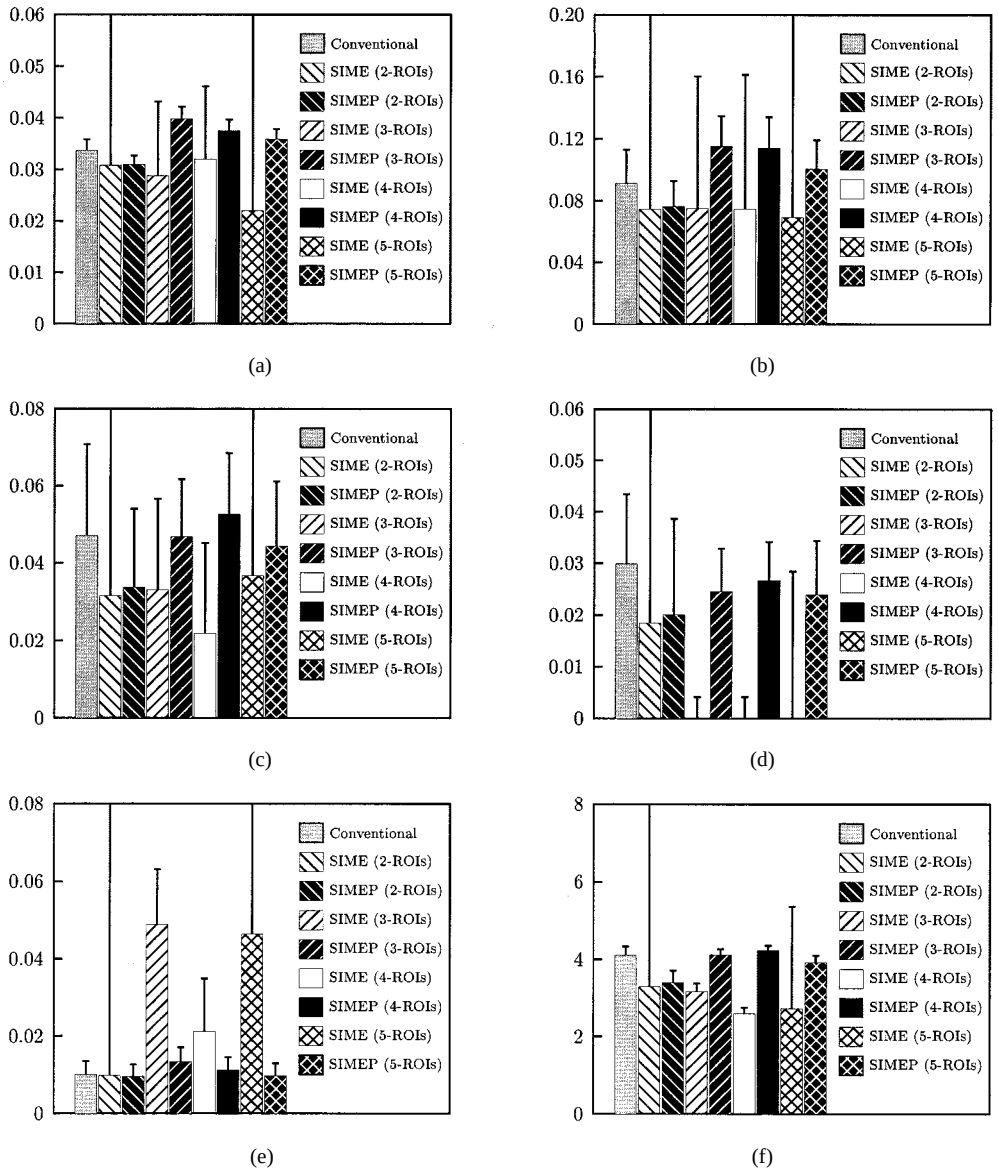

Fig. 6. Parameter estimates obtained with SIME, SIMEP, and the conventional kinetic method in WM. (a) $k_1^*\,(\mathrm{min}^{-1})$. (b) $k_2^*\,(\mathrm{min}^{-1})$. (c) $k_3^*\,(\mathrm{min}^{-1})$. (d) $k_4^*\,(\mathrm{min}^{-1})$. (e) CBV (mL/100 g). (f) rCMRGlc (mg/min/100 mL). In (a)–(f), error bars represent the SDs of the parameter estimates.

TABLE III
COMPARISON OF THE COEFFICIENTS OF VARIATION (IN PERCENTAGE) FOR rCMRGlc ESTIMATES IN TEN ROIs, OBTAINED WITH THE MEASURED ARTERIAL BLOOD SAMPLES AS THE INPUT FUNCTION AND THE RECOVERED INPUT FUNCTION OBTAINED WITH SIME (USING THREE ROIs) FOR THE THREE HUMAN SUBJECTS

PET Study	Input	BG	CBL	ITG	OAC	PA	ST	SF	TH	VC	CG
Subject 1	Measured	12.93	12.64	19.11	8.74	5.87	16.75	12.69	11.59	7.64	14.17
	Recovered	12.04	11.59	16.75	8.31	6.16	15.04	12.19	11.55	7.78	13.00
Subject 2	Measured	8.46	9.28	19.68	12.92	14.55	19.33	9.96	13.35	14.39	18.24
	Recovered	7.21	9.71	19.08	13.23	13.50	18.52	9.20	12.54	13.15	19.76
Subject 3	Measured	8.55	6.63	26.04	13.82	7.46	13.37	5.90	16.69	9.20	15.24
	Recovered	8.07	6.20	21.76	13.13	6.85	14.91	6.35	17.28	9.16	14.19

function with its initial shape rising edge followed by a rapid decline means that the difference between the measured data and fitted curves could be quite large, although the actual fitting is extremely good. Therefore, direct comparisons of the difference between the measured and fitted curves in the early time may not be the most appropriate means to show the goodness of fit. In this case, it is better to use the areas covered by the measured and the recovered input functions for comparison. In our study, we found that the areas under the estimated and measured blood curves (AUCs) at different time intervals were generally in very good agreement. However, the AUCs for the time interval of 0–2 min were underestimated or overestimated oc-

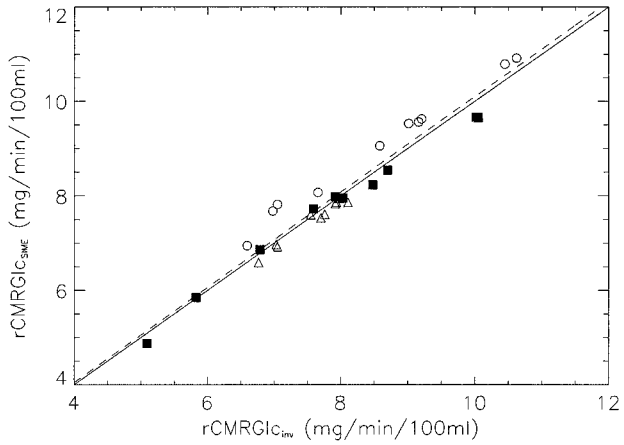

Fig. 7. Regression results of the rCMRGlc estimated using the measured arterial blood samples as the input function (*gold standard*, but invasive) and the recovered input function obtained with SIME (using three ROIs) for the three human subjects. The horizontal axis is the estimated rCMRGlc using the measured arterial blood samples as the input function ($\mathrm{rCMRGlc_{inv}}$), while the vertical axis is the one using the recovered input function obtained with SIME ($\mathrm{rCMRGlc_{SIME}}$). In this figure, the solid line represents the line of identity and the dashed line represents the line of regression. The regression line is given by $\mathrm{rCMRGlc_{SIME}} = 1.009 \times \mathrm{rCMRGlc_{inv}} + 0.007$.

casionally, due to the underestimation or overestimation of the peaks (around 15–30-s postinjection). In spite of this discrepancy, the recovered input functions were in very good agreement with the measured arterial blood samples.

Our results suggest that if the PET data are very noisy, SIME may not be able to provide acceptable estimates of CVs (or SDs) for the parameter estimates. The poor estimates may be caused by using an unstable information matrix to calculate the SD of the parameters, different orders of sensitivity functions of the output with respect to the input function model parameters, nonlinearity of the parameter space, and the dimension of the parameter space, which is very large, as well as inherent noise in the raw data. In this case, SIMEP should be applied to calculate the parameter SDs, whereby the estimated input function and the individual tissue TACs are used to perform parameter estimation separately. We have demonstrated that this provides parameter estimates and SDs, which are in good agreement with those given by the conventional kinetic method.

Similar to the conventional compartmental model fitting approach, we found that the poorest parameter estimates are obtained for k_4^* and CBV. This occurs particularly in low-activity regions such as WM, where there was considerable underestimation of k_4^* and overestimation of CBV. Nevertheless, rCMRGlc can still be estimated very reliably with the proposed methods, even when poor estimates were obtained for individual microparameters (rate constants) and the peak of the input function was not estimated accurately. This is because the value of the macro-parameter K converges rapidly and it is insensitive to the exact fitting results of $k_1^* - k_4^*$ [4]. Furthermore, although it is sensitive to the total AUC covered by the input function, it is relatively insensitive to the peak height of the input function and, therefore, the error of the rCMRGlc estimates was not significant [13].

It is expected that the parameter-estimation results should become more reliable if the kinetics of the TACs of the selected regions are sufficiently different. The ROIs used in each of the studies were defined and the degree of difference was identified *a priori*. We found that SIME was not able to provide reliable parameter estimates if ROIs whose associated TACs have similar kinetics were used in the fitting procedure due to lack of independence of measurements. In this case, where there is difficulty in selecting ROIs of different kinetic behavior, some other statistical techniques, such as cluster analysis, may be helpful to automatically identify a finite number of TACs of different kinetic characteristics present in the raw PET data. We are currently exploring such an approach.

The accuracy of parameter estimation did not improve noticeably when more than three ROIs were used. Indeed, in some cases, the results obtained using more than three ROIs were poorer than those obtained using three ROIs. We believe this is because: 1) the additional measurements do not provide additional independent information since the ROIs have similar kinetics and 2) the computational complexity and dimensions of the error surface, which define the parameter set, increase with an increasing number of ROIs. The increase in computational complexity and dimensionality of the error surface may not possess a linear relationship with the increased amount of information provided by the additional ROIs. Thus, there appears to be an optimum number of ROIs, which should be sufficient to provide new information beyond which the estimation task becomes overdetermined. We found that the optimal number of ROIs used for parameter estimation is three, which is in agreement with our results from computer simulation [9]. However, the optimal number of ROIs used in the parameter estimation procedure may be different for different individuals. Tissue heterogeneity may be another reason for the estimation results deteriorating as more ROIs are added. It has been reported that biased parameter estimates are obtained when a homogeneous tissue kinetic model (e.g., our selected model) is applied to heterogeneous tissue kinetics [15], [16].

When compared to the work of Takikawa *et al.* [7] and Eberl *et al.* [8], our method has the advantage that the kinetic model parameters $k_1^* - k_4^*$ and CBV and the input function can be estimated simultaneously with the same number of blood samples. In addition, both Takikawa *et al.* and Eberl *et al.* used the autoradiographic method to quantify rCMRGlc, and this approach assumes certain values for the kinetic model parameters, which may lead to errors in estimating rCMRGlc [3], [4], [17]. Another potential advantage of our approach is that it can be applied to other tracers, provided that the input function model can be demonstrated to be sufficiently general.

The ideal situation would be if blood sampling could be eliminated totally. However, at least one, and ideally two blood samples are required to determine plasma glucose concentration for the calculation of rCMRGlc [4]. We also found that the two late venous blood samples generally improved the performance of our method. Thus, it is likely that some blood samples will always be required for the calculation of rCMRGlc with FDG PET. Importantly, venous blood sampling is much better tolerated by patients, as it avoids the potential complications of arterial cannulation, fewer blood samples need to be taken, and there is reduced radiation exposure to the staff who perform the PET scans. Our results have encouraged us to proceed to full clinical validation of the technique.

V. Conclusions

In this paper, we validated a technique that we proposed previously for noninvasive quantification of neurologic dynamic FDG PET studies in humans. The method uses two late venous blood samples, which is minimally invasive and also markedly reduces radiation exposure to staff. We also proposed and validated a post-estimation technique, which can be applied to improve estimation of parameter variance (or numerical identifiability) when the raw PET data are noisy. Our results demonstrated that the input function can be recovered accurately from two or more ROIs and no significant difference was found between rCMRGlc estimated by our methods and the gold standard method of arterial blood sampling. The proposed methods are expected to be applicable to other tracers used in a wide range of kinetic PET studies.

Acknowledgment

The authors would like to thank the National PET/Cyclotron Center, Taipei Veterans General Hospital, Taiwan, R.O.C., for providing the brain data sets used in this paper.

References

[1] L. Sokoloff, M. Reivich, C. Kennedy, M. H. DesRosiers, C. S. Patlak, K. D. Pettigrew, D. Kakurada, and M. Shinohara, "The [^{14}C] deoxyglucose method for the measurement of local cerebral glucose utilization: Theory, procedure and normal values in the conscious and anesthetized albino rat," *J. Neurochem.*, vol. 28, pp. 897–916, 1977.

[2] M. Reivich, D. E. Kuhl, A. Wolf, J. H. Greenberg, M. E. Phelps, T. Ido, V. Casella, J. Fowler, E. J. Hoffman, A. Alavi, P. Som, and L. Sokoloff, "The [^{18}F] fluorodeoxyglucose method for the measurement of local cerebral glucose utilization in man," *Circ. Res.*, vol. 44, pp. 127–137, 1979.

[3] M. E. Phelps, S. C. Huang, E. J. Hoffman, C. Selin, L. Sokoloff, and D. E. Kuhl, "Tomographic measurement of local cerebral glucose metabolic rate in humans with (F-18)2-fluoro-2-deoxy-D-glucose: Validation of method," *Annu. Neurol.*, vol. 6, pp. 371–388, 1979.

[4] S. C. Huang, M. E. Phelps, E. J. Hoffman, K. Sideris, C. Selin, and D. E. Kuhl, "Noninvasive determination of local cerebral metabolic rate of glucose in man," *Amer. J. Physiol.*, vol. 238, pp. E69–E82, 1980.

[5] J. Correia, "A bloody future for clinical PET?," *J. Nucl. Med.*, vol. 33, pp. 620–622, 1992.

[6] R. L. Phillips, C. Y. Chen, D. F. Wong, and E. D. London, "An improved method to calculate cerebral metabolic rates of glucose using PET," *J. Nucl. Med.*, vol. 36, no. 9, pp. 1668–1679, 1995.

[7] S. Takikawa, V. Dhawan, P. Spetsieris, W. Robeson, T. Chaly, R. Dahl, D. Margouleff, and D. Eidelberg, "Noninvasive quantitative fluorodeoxyglucose PET studies with an estimated input function derived from a population-based arterial blood curve," *Radiology*, vol. 188, pp. 131–136, 1993.

[8] S. Eberl, A. R. Anayat, R. R. Fulton, P. K. Hooper, and M. J. Fulham, "Evaluation of two population-based input functions for quantitative neurological FDG PET studies," *Eur. J. Nucl. Med.*, vol. 24, no. 3, pp. 299–304, 1997.

[9] D. Feng, K. P. Wong, C. M. Wu, and W. C. Siu, "A technique for extracting physiological parameters and the required input function simultaneously from PET image measurements: Theory and simulation study," *IEEE Trans. Inform. Technol. Biomed.*, vol. 1, pp. 243–254, Dec. 1997.

[10] A. Kato, M. Diksic, Y. L. Yamamoto, S. C. Strother, and W. Feindel, "Approach for measurement of regional cerebral rate constants in the deoxyglucose method with positron emission tomography," *J. Cerebral Blood Flow Metabol.*, vol. 4, pp. 555–563, 1984.

[11] R. A. Hawkins, M. E. Phelps, and S. C. Huang, "Effects of temporal sampling, glucose metabolic rates, and disruptions of the blood-brain barrier on the FDG model with and without a vascular compartment: Studies in human brain tumors with PET," *J. Cerebal Blood Flow Metabol.*, vol. 6, pp. 170–183, 1986.

[12] D. Feng, S. C. Huang, and X. Wang, "Models for computer simulation studies of input functions for tracer kinetic modeling with positron emission tomography," *Int. J. Biomed. Comput.*, vol. 32, pp. 95–110, 1993.

[13] A. Kato, D. Menon, M. Diksic, and Y. L. Yamamoto, "Influence of the input function on the calculation of the local cerebral metabolic rate for glucose in the deoxyglucose method," *J. Cerebral Blood Flow Metabol.*, vol. 4, pp. 41–46, 1984.

[14] K. Chen, S. C. Huang, and D. C. Yu, "The effects of measurement errors in plasma radioactivity curve on parameter estimation in positron emission tomography," *Phys. Med. Biol.*, vol. 36, no. 9, pp. 1183–1200, 1991.

[15] K. Herholz and C. S. Patlak, "The influence of tissue heterogeneity on results of fitting nonlinear model equations to regional tracer uptake curves: with an application to compartmental models used in positron emission tomography," *J. Cerebral . Blood Flow Metabol.*, vol. 7, pp. 214–229, 1987.

[16] K. Schmidt, G. Lucignani, R. M. Moresco, G. Rizzo, M. C. Gilardi, C. Messa, F. Colombo, F. Fazio, and L. Sokoloff, "Errors introduced by tissue heterogeneity in estimation of local cerebral glucose utilization with current kinetic models of the [^{18}F]fluorodeoxyglucose method," *J. Cerebral Blood Flow Metabol.*, vol. 12, pp. 823–834, 1992.

[17] S. C. Huang, M. E. Phelps, E. J. Hoffman, and D. E. Kuhl, "Error sensitivity of fluorodeoxyglucose method for measurement of cerebral metabolic rate of glucose," *J. Cerebral Blood Flow Metabol.*, vol. 1, pp. 391–401, 1981.

Koon-Pong Wong (M'00) was born in Hong Kong. He received the B.Eng. degree (with first class honors) in electronic engineering and the Ph.D. degree in electronic and information engineering from the Hong Kong Polytechnic University, Hong Kong, in 1996 and 1999, respectively.

In August 1999, he joined the Basser Department of Computer Science, The University of Sydney, Sydney, Australia, where he is currently a Post-Doctoral Research Associate. He is also a Post-Doctoral Scientist in the Department of PET and Nuclear Medicine, Royal Prince Alfred Hospital, Sydney, Australia. He was a Visiting Scholar at the Basser Department of Computer Science, The University of Sydney, from 1996 to 1997. His research interests include noninvasive methodology for quantitative PET, modeling and simulation, fast computational algorithms, and signal processing.

(David) Dagan Feng (S'88–M'88–SM'94) received the M.E. degree in electrical engineering and computing science from the Shanghai JiaoTong University, Shanghai, China, in 1982, and the M.Sc. degree in biocybernetics and Ph.D. degree in computer science from the University of California at Los Angeles (UCLA), in 1985 and 1988, respectively.

After briefly being an Assistant Professor at the University of California, Riverside, he joined the Department of Computer Science, The University of Sydney, Sydney, Australia, at the end of 1988, as Lecturer, Senior Lecturer, Reader, and then Professor, and is currently the Head of this department. Since 1997, he has also been a Professor in the Department of Electronic and Information Engineering, Hong Kong Polytechnic University, Hong Kong. He is Founder and Director of the Biomedical and Multimedia Information Technology (BMIT) Group, The University of Sydney. He is also Deputy Director of the Center for Multimedia Signal Processing (CMSP), Hong Kong Polytechnic University. He is also an Honorary Research Consultant at the Royal Prince Alfred Hospital, Sydney, Australia, as well as Guest Professor at Northwestern Polytechnic University, Shanghai JiaoTong University, and Tsinghua University. His research interests include biomedical and multimedia information technology, functional imaging, modeling and simulation, fast algorithms, and data compression. He has authored or co-authored over 100 scholarly research papers and has made several landmark contributions in his field.

Dr. Feng has been a special area editor for the IEEE TRANSACTIONS ON INFORMATION TECHNOLOGY IN BIOMEDICINE, guest editor for the IEEE TRANSACTIONS ON INFORMATION TECHNOLOGY IN BIOMEDICINE Special Issue on "Multimedia Information Technology in Biomedicine," vice-chair of the International Federation of Automatic Control (IFAC) Technical Committee on BIOMED, and chairman of the Hong Kong Institution of Engineers (HKIE) Biomedical Division. He has been an invited keynote speaker for a number of major international conferences, including the IEEE ITAB'99, Washington, DC, the most prestigious conference for information technology (IT) applications in biomedicine. He has received a number of awards, including the Crump Prize for Excellence in Medical Engineering from the USA and 14 technical innovation awards during the period when he worked in industry.

Steven R. Meikle (M'96–SM'00) received the B.AppSc. degree in applied physics from the University of Technology, Sydney, Australia, in 1987, and the Ph.D. degree in biomedical engineering from the University of New South Wales, Sydney, Australia, in 1994.

He is currently a Principal Scientific Officer in the Department of PET and Nuclear Medicine, Royal Prince Alfred Hospital (RPAH), Sydney, Australia, and an Honorary Research Associate in the Basser Department of Computer Science, The University of Sydney, Sydney, Australia. He possesses over 12 years experience in the field, including research appointments at two leading PET facilities—the University of California at Los Angeles (UCLA) School of Medicine PET Center and the MRC Cyclotron Unit, Hammersmith Hospital, London, U.K. He has established strong collaborative links with these institutions, as well as the leading PET scanner manufacturer, CTI/Siemens and, more recently, the Detector Group, Thomas Jefferson National Accelerator Facility. His research interests include the development of imaging instrumentation, image reconstruction algorithms, and tracer kinetic modeling. He has made several outstanding contributions to the field that have contributed to the international reputation of the RPAH Physics Group, which include the scanning transmission line source for single photon emission computed tomography (SPECT), transmission-based scatter correction, and simultaneous emission and transmission PET scanning. He has authored or co-authored over 40 papers in peer-reviewed journals.

Dr. Meikle serves on the IEEE Radiation Instrumentation Advisory Committee and the Federal Committee of the Australian and New Zealand Society of Nuclear Medicine. He was the recipient of the 1994 Boyce Worthley Award presented by the Australasian College of Physical Scientists and Engineers in Medicine.

Michael J. Fulham received the M.B.B.S. degree (with honors) from the University of New South Wales, Sydney, Australia, in 1979.

He completed his internal medicine and neurology training in 1987 at the Royal Prince Alfred (RPA) Hospital, Sydney, Australia. He was admitted to the Fellowship of the Royal Australasian College of Physicians (FRACP) in 1985. In 1988, he joined the Neuroimaging Branch of the National Institute of Neurological and Communicative Disorders and Stroke (NINCDS), National Institutes of Health (NIH), Bethesda, MD, where he carried out research in the neurosciences for five years. While with the NIH, he became a recognized authority on PET and magnetic resonance (MR) spectroscopy in neurooncology with many invited overseas presentations. He returned to Australia in 1993 as a Staff Neurologist and was placed in charge of the PET Program at the RPA Hospital, which was one of only two PET programs in the country. In 1997, he became the Director of the Department of PET and Nuclear Medicine, RPA, and Associate Professor in the Department of Medicine, The University of Sydney, Sydney, Australia. In 2000, he became the Area Clinical Director of Medical Imaging Services for the Central Sydney Area Health Service, of which RPA is the flagship. His research interests are in the application of functional imaging to the neurosciences, in particular, for brain tumors and neurodegenerative conditions. He has also overseen the development of a strong clinical and research teams in PET, as it has expanded into many areas of oncology where it has made significant impact on clinical management. He was awarded the 1992 NIH Merit Award for Outstanding Performance in Research.